Geochemistry summary[1]

K.M. Gillis, J.E. Snow, A. Klaus, G. Guerin, N. Abe, N. Akizawa, G. Ceuleneer, M.J. Cheadle, Á. Adrião, K. Faak, T.J. Falloon, S.A. Friedman, M.M. Godard, Y. Harigane, A.J. Horst, T. Hoshide, B. Ildefonse, M.M. Jean, B.E. John, J.H. Koepke, S. Machi, J. Maeda, N.E. Marks, A.M. McCaig, R. Meyer, A. Morris, T. Nozaka, M. Python, A. Saha, and R.P. Wintsch[2]

Chapter contents

[1]Gillis, K.M., Snow, J.E., Klaus, A., Guerin, G., Abe, N., Akizawa, N., Ceuleneer, G., Cheadle, M.J., Adrião, Á., Faak, K., Falloon, T.J., Friedman, S.A., Godard, M.M., Harigane, Y., Horst, A.J., Hoshide, T., Ildefonse, B., Jean, M.M., John, B.E., Koepke, J.H., Machi, S., Maeda, J., Marks, N.E., McCaig, A.M., Meyer, R., Morris, A., Nozaka, T., Python, M., Saha, A., and Wintsch, R.P., 2014. Geochemistry summary. *In* Gillis, K.M., Snow, J.E., Klaus, A., and the Expedition 345 Scientists, *Proc. IODP,* 345: College Station, TX (Integrated Ocean Drilling Program).
doi:10.2204/iodp.proc.345.114.2014
[2]Expedition 345 Scientists' addresses.

Introduction

A representative suite of the lithologies recovered at Site U1415 were analyzed during Integrated Ocean Drilling Program (IODP) Expedition 345 (see "Igneous petrology" and "Metamorphic petrology" in each hole chapter for characterization of the lithologic units). Chemical analyses were performed on 3 basaltic samples from Holes U1415J and U1415N; 45 gabbroic samples from Holes U1415E, U1415H–U1415J, and U1415P; and 5 samples of drilling-induced disaggregated gabbro from Holes U1415I and U1415J. Sample selection was based on discussion among representatives from all expertise groups within the shipboard scientific party. Inductively coupled plasma–atomic emission spectroscopy was used to determine major and trace element concentrations, and gas chromatography was used to measure H_2O, CO_2, and S concentrations. Geochemical data are reported in Table T1. These concentrations are reported on a volatile-free basis for major and trace elements.

The results of the chemical study are described in detail in "Inorganic geochemistry" in each hole chapter; the main results and petrogenetic outcomes are summarized below. Drilling-induced disaggregated gabbro samples were not included in this summary because they showed evidence of contamination by drilling materials (e.g., antirust coatings and components of the drill bit in Hole U1415I and drilling mud in Hole U1415J).

Basalt

Site U1415 basalt has a composition similar to the primitive mid-ocean-ridge basalt (MORB) previously sampled in the Hess Deep area at Ocean Drilling Program (ODP) Leg 147 Site 894 (Shipboard Scientific Party, 1993). In detail, Site U1415 basalt composition is reflective of its petrography, in particular for the sparsely to moderately phyric Hole U1415N basalt. Overall, Site U1415 basalt plots at the most depleted end of the East Pacific Rise (EPR) basalt field (e.g., Allan et al., 1996) with high Mg# (69; 100 × cationic Mg/[Mg + Fe] with all Fe as Fe^{2+}) in Hole U1415J aphyric basalt, low TiO_2 (<1.2 wt%), and lithophile trace element contents (e.g., Y = 21–27 ppm).

Gabbroic rock

During Expedition 345, 1 gabbronorite sample from Hole U1415E, 4 clinopyroxene oikocryst-bearing troctolite samples and gabbro samples from Holes U1415I and U1415J, 9 orthopyroxene-bearing olivine gabbro and olivine-bearing gabbronorite samples from Holes U1415H–U1415J and U1415P, 10 troctolite samples from Holes U1415J and U1415P, and 20 olivine gabbro and gabbro samples from Holes U1415J and U1415P were selected for chemical analyses (Table **T1**). Except for the gabbronorite in Hole U1415E, all samples are characterized by their significantly less evolved composition compared to gabbroic rock previously collected along the Northern Escarpment of the Hess Deep Rift (Gillis, Mével, Allan, et al., 1993; Pedersen et al., 1996; Natland and Dick, 1996; Hanna, 2004; Kirchner and Gillis, 2012). The rocks overlap in composition with the most primitive gabbro and troctolite sampled along the EPR (Pito Deep; Perk et al., 2007) (Figs. **F1, F2;** see also "Inorganic geochemistry" for each hole). The main chemical signatures of the different gabbroic rocks sampled at Site U1415 and of the alteration that affected the lithologic intervals are summarized below.

Hole U1415E gabbronorite

Hole U1415E gabbronorite has low Mg# (73) and low Cr (123 ppm) and Ni (67 ppm) concentrations and plots at the most primitive end of the field of gabbro and gabbronorite previously sampled at Hess Deep. These compositions indicate that this sample crystallized within an evolved magmatic system, late in a MORB crystallization sequence.

Site U1415 primitive gabbroic series

Olivine gabbro and gabbro

The olivine gabbro and gabbro sampled in Holes U1415J and U1415P have compositions typical of primitive gabbroic rocks (e.g., Cannat, Karson, Miller, et al., 1995; Godard et al., 2009; Perk et al., 2007). They have high Mg# (79–87) and Ca# (100 × cationic Ca/[Ca + Na]; 77–92), high Ni contents (130–570 ppm), and low TiO_2 (0.1–0.3 wt%) and incompatible lithophile element (e.g., Y < 11 ppm) contents. Six samples are distinguished by a significantly higher Cr content (1500–2550 ppm) compared to neighboring gabbro. These high concentrations may reflect the occurrence of a Cr-rich minor phase (e.g., Cr-spinel) in these samples (see "**Igneous petrology**" in the "Hole U1415P" chapter [Gillis et al., 2014]).

Clinopyroxene oikocryst-bearing troctolite and gabbro

Although they are very different texturally, clinopyroxene oikocryst-bearing troctolite and gabbro sampled in Holes U1415I and U1415J are similar in composition to Site U1415 olivine gabbro in that they have high Mg# (80–85) and Ca# (82–86), high Ni concentrations (150–330 ppm), and low TiO_2 (<0.2 wt%) and trace element (e.g., Y < 6 ppm) contents.

Orthopyroxene-bearing olivine gabbro and olivine-bearing gabbronorite

Orthopyroxene-bearing olivine gabbro has primitive compositions similar to neighboring gabbro and olivine gabbro in that it is characterized by high Mg# (79–87) and Ca# (73–92) and low TiO_2 (0.1–0.3 wt%) and trace element (e.g., Y < 6 ppm) contents. Gabbro has high Ni (150–460 ppm) and Cr (222–1000 ppm) contents typical of primitive oceanic gabbro (e.g., Fig. **F1**).

Troctolite

Troctolite overlaps in composition with gabbro but has on average a more primitive composition with high Mg# (81–89) and Ca# (79–98), high Ni (260–1500 ppm) and Cr (365–1100 ppm) contents, and low TiO_2 (<0.1 wt%) and incompatible lithophile element (e.g., Y < 3 ppm) contents. The most primitive troctolite sampled in Hole U1415P has a composition that overlaps the field of impregnated mantle peridotite from the Hess Deep Rift and elsewhere (Fig. **F1**). However, in contrast to the olivine-rich troctolite sampled at Atlantis Massif (IODP Expedition 304/305 Site U1309), these samples are low in Ni relative to their high Mg#, which suggests that they were formed by a dominantly cumulate process. Our data provide the first chemical characterization of these rock types in the Hess Deep area.

Alteration

Measured volatiles demonstrate a progressive degree of alteration within all studied samples. Gabbro has loss on ignition (LOI) values from 1.1 to 5.3 wt%, and troctolite has LOI values from 2.7 to 9.7 wt% (Table **T1**). The combined contents of H_2O (but not CO_2) are in good agreement with the LOI values. The dominant volatile component within Site U1415 plutonic rock is bound water or hydroxyl in secondary alteration phases. Positive correlations between H_2O, optically quantified olivine, and Ni, a trace element compatible in olivine, point toward serpentinization as the dominant alteration process affecting the composition of the drilled troctolitic and gabbroic intervals. Apart from water addition, our data do not provide evidence of systematic elemental mobility caused by alteration. No parallels between CaO (prehnite) and/or Al_2O_3 (prehnite/chlorite) and H_2O were observed. Also, the studied samples have no substantial amounts of CO_2. Correlations between secondary sulfide minerals and the S abundances were not observed because of small-scale heterogeneities in the distribution of these minerals.

Comparison to previously sampled oceanic gabbro

The main geochemical characteristics of Site U1415 gabbroic rocks are consistent with formation as a cumulate sequence from a common parental MORB melt, with troctolite representing the most primitive end-member of this sequence. Site U1415 gabbroic rocks appear to constitute a suite of gabbroic rocks of which the gabbronorite sampled in Hole U1415E represents the most evolved end-member. The rocks overlap in composition with the most primitive of slow- and fast-spread gabbroic rock sequences (Figs. **F1**, **F2**). These primitive geochemical signatures seem, however, to be contradictory with orthopyroxene (as much as 5%) in the primary mineral assemblage of the olivine gabbro sampled in Holes U1415I, U1415J, and U1415P. In MORB crystallization series, orthopyroxene is expected to crystallize from evolved melts. The presence of orthopyroxene in the primitive gabbroic sequence sampled at Site U1415 suggests that it was formed in a more complex magmatic system.

A single sample of primitive gabbroic rock containing high-Mg# orthopyroxene was sampled along the southern slope of the intrarift ridge in the Hess Deep area (Coogan et al., 2002). The Hess Deep sample was interpreted as indicating that a fraction of the melts that formed the lower crust interacted with the mantle during melt extraction and therefore was not undersaturated in orthopyroxene, as are typical MORB parental melts. High-Mg# depleted gabbronorite has also been observed in Oman ophiolite (Boudier et al., 2000) and at Deep Sea Drilling Project Site 334 on the Mid-Atlantic Ridge (Nonnotte et al., 2005), where they were interpreted as resulting from the contamination of MORB parental melts by water. Further studies will be carried out on shore to decipher the petrogenetic processes leading to the formation of the orthopyroxene-bearing primitive gabbro sampled during Expedition 345.

As noted above, Site U1415 gabbroic rocks have compositions similar to Pito Deep gabbro and troctolite (Perk et al., 2007). High-Mg# plutonic rock from Pito Deep has been sampled between 300 and 700 m beneath the sheeted dike complex (Perk et al., 2007), including a single layered specimen. Site U1415 gabbroic rock is drilled from a deeper oceanic crustal section and display extensive modal layering and primitive geochemistry. In the last decades, countless studies of layered intrusions have cast light on a wide variety of layer-forming mechanisms that influence the cumulate geochemistry (e.g., Holness and Winpenny, 2009; Meyer et al., 2009). However, modal layering in MORB cumulates from fast-spreading ridges, as well as their actual composition, remains nearly unknown, and it is worthwhile to note that fast-spreading plutonic crust remains undersampled compared to slow-spreading crust, as illustrated in Figures **F1** and **F2**.

References

Bodinier, J.-L., and Godard, M., 2003. Orogenic, ophiolitic, and abyssal peridotites. *Treatise Geochem.,* 2:1–73. **doi:10.1016/B0-08-043751-6/02004-1**

Boudier, F., Godard, M., and Armbruster, C., 2000. Significance of gabbronorite occurrence in the crustal section of the Semail ophiolite. *Mar. Geophys. Res.,* 21(3–4):307–326. **doi:10.1023/A:1026726232402**

Cannat, M., Karson, J.A., Miller, D.J., et al., 1995. *Proc. ODP, Init. Repts.,* 153: College Station, TX (Ocean Drilling Program). **doi:10.2973/odp.proc.ir.153.1995**

Coogan, L.A., Gillis, K.M., MacLeod, C.J., Thompson, G.M., and Hékinian, R., 2002. Petrology and geochemistry of the lower ocean crust formed at the East Pacific Rise and exposed at Hess Deep: a synthesis and new results. *Geochem., Geophys., Geosyst.,* 3(11):8604. **doi:10.1029/2001GC000230**

Dick, H.J.B., Natland, J.H., Miller, D.J., et al., 1999. *Proc. ODP, Init. Repts.,* 176: College Station, TX (Ocean Drilling Program). **doi:10.2973/odp.proc.ir.176.1999**

Expedition 304/305 Scientists, 2006. Site U1309. *In* Blackman, D.K., Ildefonse, B., John, B.E., Ohara, Y., Miller, D.J., MacLeod, C.J., and the Expedition 304/305 Scientists, *Proc. IODP,* 304/305: College Station, TX (Integrated Ocean Drilling Program Management International, Inc.). **doi:10.2204/iodp.proc.304305.103.2006**

Gillis, K., Mével, C., Allan, J., et al., 1993. *Proc. ODP, Init. Repts.,* 147: College Station, TX (Ocean Drilling Program). **doi:10.2973/odp.proc.ir.147.1993**

Gillis, K.M., Snow, J.E., Klaus, A., Guerin, G., Abe, N., Akizawa, N., Ceuleneer, G., Cheadle, M.J., Adrião, Á., Faak, K., Falloon, T.J., Friedman, S.A., Godard, M.M., Harigane, Y., Horst, A.J., Hoshide, T., Ildefonse, B., Jean, M.M., John, B.E., Koepke, J.H., Machi, S., Maeda, J., Marks, N.E., McCaig, A.M., Meyer, R., Morris, A., Nozaka, T., Python, M., Saha, A., and Wintsch, R.P., 2014. Hole U1415P. *In* Gillis, K.M., Snow, J.E., Klaus, A., and the Expedition 345 Scientists, *Proc. IODP,* 345: College Station, TX (Integrated Ocean Drilling Program). doi:10.2204/iodp.proc.345.113.2014

Godard, M., Awaji, S., Hansen, H., Hellebrand, E., Brunelli, D., Johnson, K., Yamasaki, T., Maeda, J., Abratis, M., Christie, D., Kato, Y., Mariet, C., and Rosner, M., 2009. Geochemistry of a long in-situ section of intrusive slow-spread oceanic lithosphere: results from IODP Site U1309 (Atlantis Massif, 30°N Mid-Atlantic-Ridge). *Earth Planet. Sci. Lett.,* 279(1–2):110–122. doi:10.1016/j.epsl.2008.12.034

Hanna, H.D., 2004. Geochemical variations in basaltic glasses from an incipient rift and upper level gabbros from Hess Deep, eastern equatorial Pacific [M.Sc. thesis]. Duke Univ., Durham.

Hékinian, R., Bideau, D., Francheteau, J., Cheminee, J.L., Armijo, R., Lonsdale, P., and Blum, N., 1993. Petrology of the East Pacific Rise crust and upper mantle exposed in Hess Deep (eastern equatorial Pacific). *J. Geophys. Res.: Solid Earth,* 98(B5):8069–8094. doi:10.1029/92JB02072

Holness, M.B., and Winpenny, B., 2009. The Unit 12 allivalite, Eastern Layered Intrusion, Isle of Rum: a textural and geochemical study of an open-system magma chamber. *Geol. Mag.,* 146(3):437–450. doi:10.1017/S0016756808005797

Kirchner, T.M., and Gillis, K.M., 2012. Mineralogical and strontium isotopic record of hydrothermal processes in the lower ocean crust at and near the East Pacific Rise. *Contrib. Mineral. Petrol.,* 164(1):123–141 doi:10.1007/s00410-012-0729-5

Meyer, R., Nicoll, G.R., Hertogen, J., Troll, V.R., Ellam, R.M., and Emeleus, C.H., 2009. Trace element and isotope constraints on crustal anatexis by upwelling mantle melts in the North Atlantic igneous province: an example from the Isle of Rum, NW Scotland. *Geol. Mag.,* 146(3):382–399. doi:10.1017/S0016756809006244

Miller, D.J., Iturrino, G.J., and Christensen, N.I., 1996. Geochemical and petrological constraints on velocity behavior of lower crustal and upper mantle rocks from the fast-spreading ridge at Hess Deep. *In* Mével, C., Gillis, K.M., Allan, J.F., and Meyer, P.S. (Eds.), *Proc. ODP, Sci. Results,* 147: College Station, TX (Ocean Drilling Program), 477–490. doi:10.2973/odp.proc.sr.147.028.1996

Natland, J.H., and Dick, H.J.B., 2009. Paired melt lenses at the East Pacific Rise and the pattern of melt flow through the gabbroic layer at a fast-spreading ridge. *Lithos,* 112(1–2):73–86. doi:10.1016/j.lithos.2009.06.017

Nonnotte, P., Ceuleneer, G., and Benoit, M., 2005. Genesis of andesitic–boninitic magmas at mid-ocean ridges by melting of hydrated peridotites: geochemical evidence from DSDP Site 334 and gabbronorites. *Earth Planet. Sci. Lett.,* 236(3–4):632–653. doi:10.1016/j.epsl.2005.05.026

Pedersen, R.B., Malpas, J., and Falloon, T., 1996. Petrology and geochemistry of gabbroic and related rocks from Site 894, Hess Deep. *In* Mével, C., Gillis, K.M., Allan, J.F., and Meyer, P.S. (Eds.), *Proc. ODP, Sci. Results,* 147: College Station, TX (Ocean Drilling Program), 3–19. doi:10.2973/odp.proc.sr.147.001.1996

Perk, N.W., Coogan, L.A., Karson, J.A., Klein, E.M., and Hanna, H.D., 2007. Petrology and geochemistry of primitive lower oceanic crust from Pito Deep: implications for the accretion of the lower crust at the southern East Pacific Rise. *Contrib. Mineral. Petrol.,* 154(5):575–590. doi:10.1007/s00410-007-0210-z

Saunders, A.D., Fornari, D.J., Joron, J.-L., Tarney, J., and Treuil, M., 1982. Geochemistry of basic igneous rocks, Gulf of California, Deep Sea Drilling Project Leg 64. *In* Curray, J.R., Moore, D.G., et al. (Eds.), *Init. Repts. DSDP,* 64: Washington, DC (U.S. Govt. Printing Office), 595–642. doi:10.2973/dsdp.proc.64.112.1982

Shipboard Scientific Party, 1993. Site 894. *In* Gillis, K., Mével, C, Allan, J., et al., *Proc. ODP, Init. Repts.,* 147: College Station, TX (Ocean Drilling Program), 45–108. doi:10.2973/odp.proc.ir.147.103.1993

Publication: 12 February 2014
MS 345-114

Figure F1. Ca# vs. Mg# plot of compositions of recovered gabbroic rock, Site U1415. Gabbronorite and gabbro with >2% orthopyroxene (Opx) is grouped as orthopyroxene-bearing gabbro. For comparison, a compilation of plutonic rock sampled along the East Pacific Rise (EPR) at Hess Deep (Hékinian et al., 1993; Gillis, Mével, Allan, et al., 1993; Miller et al., 1996; Natland and Dick, 2009; Pedersen et al., 1996; Hanna, 2004; Kirchner and Gillis, 2012), Pito Deep (Perk et al., 2007), and other locations (Saunders et al., 1982) is shown. The range of composition of gabbro drilled in slow-spreading oceanic crust in Ocean Drilling Program (ODP) Hole 735B at Southwest Indian Ridge (Dick, Natland, Miller, et al., 1999), during ODP Leg 153 (Cannat, Karson, Miller, et al., 1995), and at Integrated Ocean Drilling Program (IODP) Site U1309 on the Mid-Atlantic Ridge (Expedition 304/305 Scientists, 2006; Godard et al., 2009) and (refractory and impregnated) abyssal peridotite (compilation of Bodinier and Godard, 2003) is also illustrated. Note that Hess Deep gabbro with a Mg# of ~72–79 has been recently analyzed (MacLeod et al., pers. comm., 2013) but was not added to the Hess Deep data set because the results are not yet published. Ol = olivine.

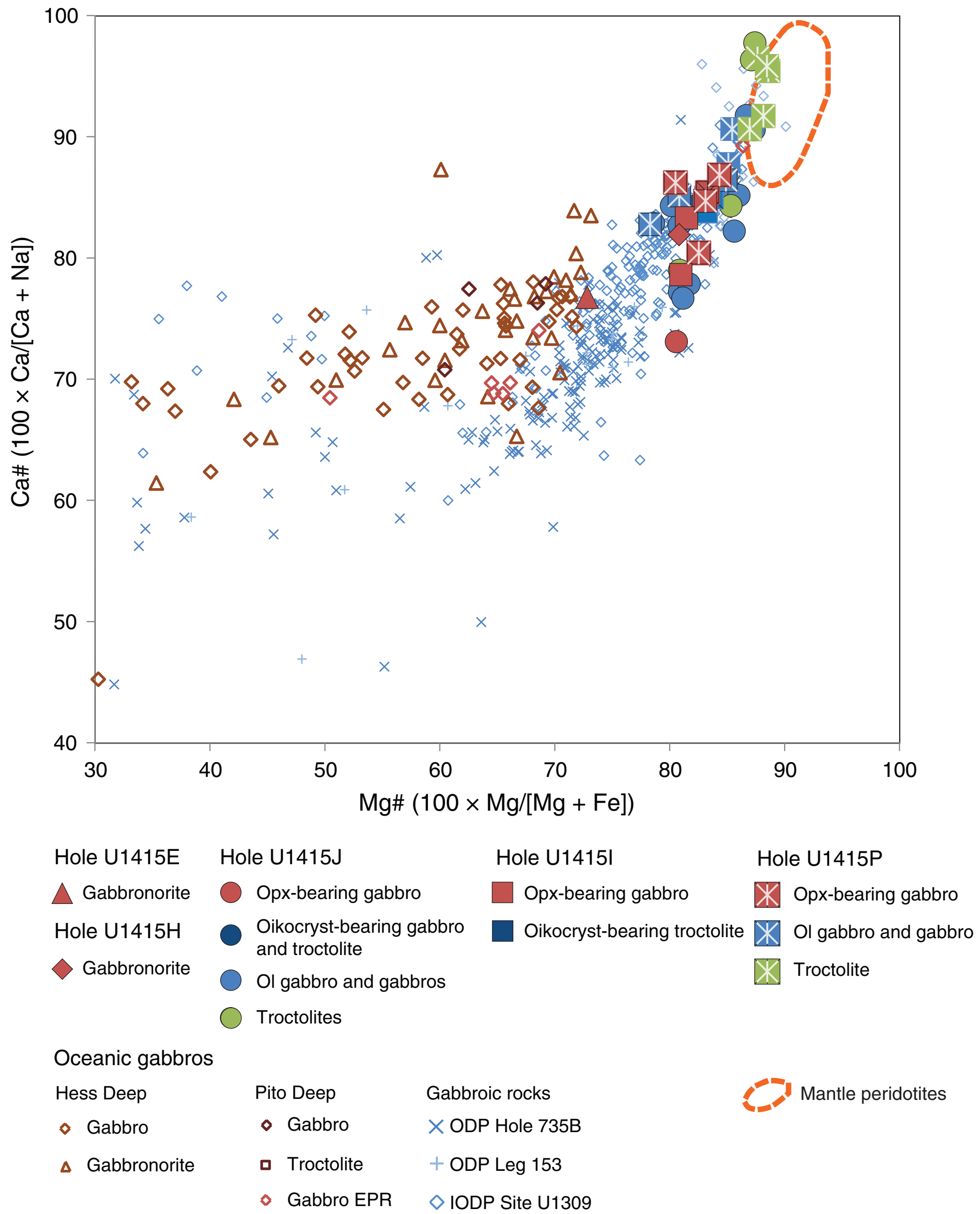

Figure F2. Ni vs. Mg# plot of compositions of recovered gabbroic rock, Site U1415. Gabbronorite and gabbro with >2% orthopyroxene (Opx) is grouped as orthopyroxene-bearing gabbro. For comparison, a compilation of plutonic rock sampled along the East Pacific Rise (EPR) at Hess Deep (Hékinian et al., 1993; Gillis, Mével, Allan, et al., 1993; Miller et al., 1996; Natland and Dick, 2009; Pedersen et al., 1996; Hanna, 2004; Kirchner and Gillis, 2012), Pito Deep (Perk et al., 2007), and other locations (Saunders et al., 1982) is shown. The range of composition of gabbro drilled in slow-spreading oceanic crust in Ocean Drilling Program (ODP) Hole 735B at Southwest Indian Ridge (Dick, Natland, Miller, et al., 1999), during ODP Leg 153 (Cannat, Karson, Miller, et al., 1995), and at Integrated Ocean Drilling Program (IODP) Site U1309 on the Mid-Atlantic Ridge (Expedition 304/305 Scientists, 2006; Godard et al., 2009) and (refractory and impregnated) abyssal peridotite (compilation of Bodinier and Godard, 2003) is also illustrated. Note that Hess Deep gabbro with a Mg# of ~72–79 has been recently analyzed (MacLeod et al., pers. comm., 2013) but was not added to the Hess Deep data set because the results are not yet published. Ol = olivine.

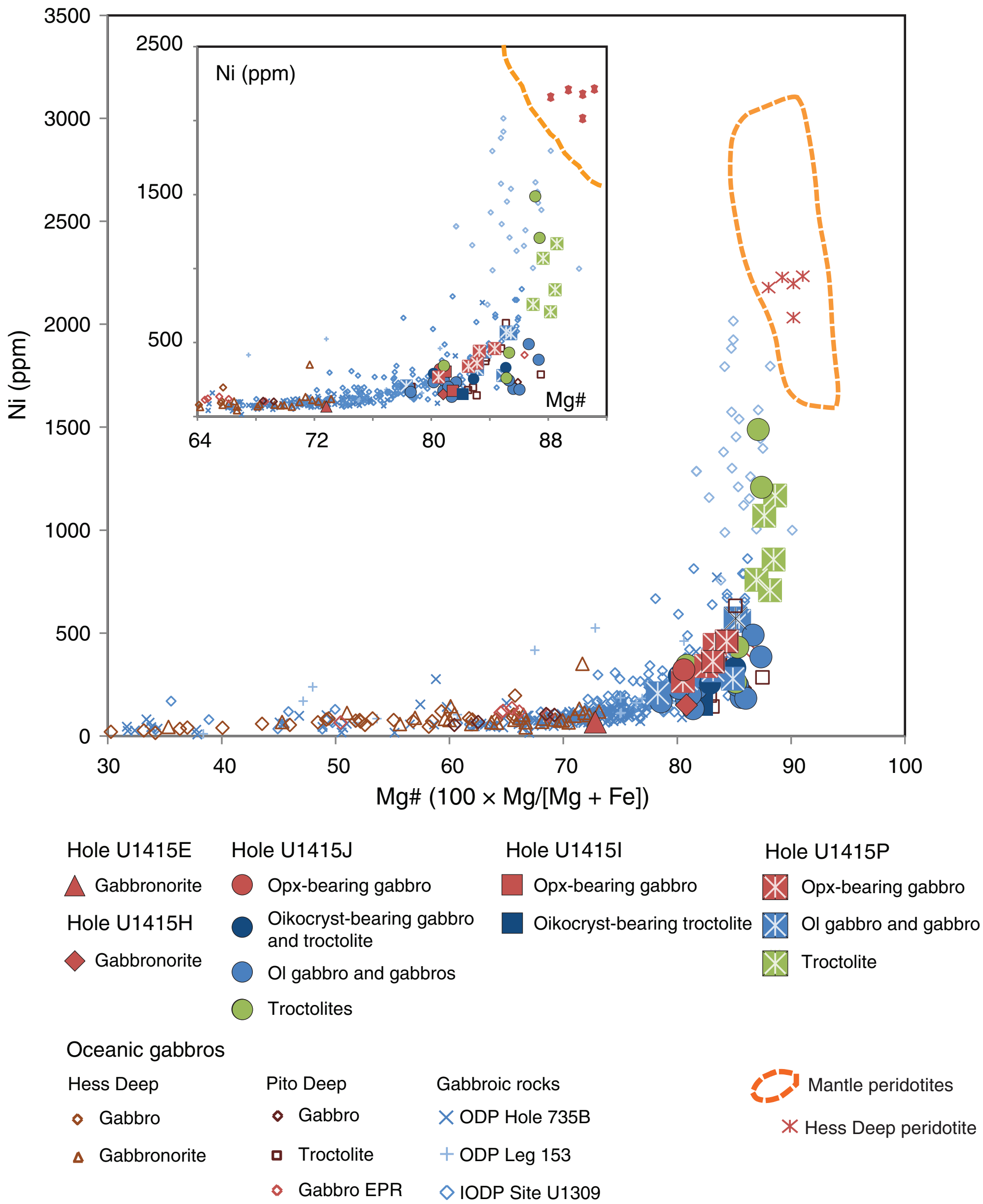

Table T1. Chemical composition of sampled rock types, Expedition 345.

Core, section, interval (cm)	Rock name	Lithologic interval	SiO_2 (wt%)	TiO_2 (wt%)	Al_2O_3 (wt%)	$Fe_2O_3{}^T$ (wt%)	MgO (wt%)	MnO (wt%)	CaO (wt%)	Na_2O (wt%)	K_2O (wt%)	P_2O_5 (wt%)	Total (wt%)	LOI (wt%)	Mg#	H_2O (wt%)	CO_2 (wt%)	S (ppm)	Sc (ppm)	V (ppm)	Cr (ppm)	Ni (ppm)	Cu (ppm)	Zn (ppm)	Sr (ppm)	Y (ppm)	Zr (ppm)	Ba (ppm)	Nb (ppm)
345-U1415E-																													
1R-1, 44–47	Gabbronorite	5	51.02	0.53	15.34	7.69	10.40	0.15	13.03	2.18	0.03	<0.07	100.35	0.44	72.8	0.95	0.09	390	43	196	123	67	47	44	69	11	<10	ND	<5
345-U1415H-																													
1R-1, 17–23	Ol-bearing gabbronorite	4	50.24	0.31	17.93	4.85	10.31	0.10	15.07	1.84	<0.1	<0.07	100.65	1.07	80.8	1.38	0.14	193	36	148	1001	150	67	28	67	5	<10	ND	<5
345-U1415I-																													
2R-1, 0–4	Opx-bearing ol gabbro	3	47.75	0.18	19.36	5.78	12.44	0.10	12.92	1.94	0.02	<0.07	100.47	3.23	81.0	3.46	0.06	559	26	100	774	304	66	33	72	4	<10	ND	<5
3R-1, 38–43	Disaggregated gabbro	4	48.77	0.44	18.02	5.47	10.48	0.11	14.23	2.49	0.06	<0.07	100.07	3.66	79.2	2.83	0.05	364	31	142	735	187	98	140	98	10	19	ND	<5
3R-2, 70–76	Disaggregated gabbro	5	49.22	0.40	18.65	5.38	10.16	0.10	14.37	2.61	0.06	<0.07	100.95	3.55	78.9	2.98	0.06	158	30	139	697	176	72	158	99	9	42	ND	<5
3R-3, 72–77	Disaggregated gabbro	6	49.39	0.42	18.77	5.46	10.36	0.10	14.25	2.63	0.08	<0.07	101.46	3.53	79.0	2.95	0.06	160	29	145	707	174	85	140	102	9	35	ND	<5
4R-1, 50–52	Ol-bearing gabbronorite	16	49.54	0.17	18.80	4.88	10.83	0.09	14.54	1.61	<0.02	<0.07	100.45	1.04	81.5	0.98	0.07	436	30	101	701	174	75	27	70	3	<20	<65	ND
4R-1, 112–114	Cpx oikocryst-bearing troctolite	22	49.41	0.16	19.23	4.21	9.77	0.08	15.77	1.63	<0.02	<0.07	100.27	1.61	82.1	1.22	0.04	293	30	94	1110	153	58	23	76	2	<20	<65	ND
345-U1415J-																													
2G-1, 0–13	Aphyric basalt	G1	49.02	1.03	16.80	8.71	9.75	0.15	12.15	2.35	<0.02	<0.07	99.96	1.86	68.9	1.78	ND	129	34	218	519	213	63	59	30	24	43	<65	ND
2G, 0–1013	Disaggregated gabbro		49.97	0.63	18.12	6.85	11.04	0.12	11.64	2.98	0.12	<0.07	101.47	3.30	76.2	3.93	0.14	438	29	147	478	150	57	62	108	13	29	69	ND
2G, 0–1013	Disaggregated gabbro		49.13	0.70	16.98	7.00	11.27	0.13	12.48	2.61	0.09	<0.07	100.40	2.67	76.1	3.42	0.07	666	35	166	638	145	66	60	87	12	32	96	ND
3R-1, 11–13	Ol-opx bearing gabbro	5	46.34	0.13	18.73	7.80	16.35	0.11	9.84	2.00	ND	<0.70	101.29	5.83	80.6	5.33	ND	382	14	75	253	320	58	45	117	2	41	ND	<5
3R-1, 21–22	Ol-bearing gabbro	6	49.24	0.22	18.35	3.48	10.46	0.08	16.40	1.96	<0.02	<0.07	100.19	2.30	85.6	1.96	ND	167	38	123	2149	187	53	14	96	4	<20	<65	ND
3R-1, 79–82	Gabbro	11	50.37	0.30	17.29	4.72	10.43	0.10	16.15	1.69	<0.02	<0.07	101.05	1.14	81.4	1.17	0.08	177	45	169	645	132	70	25	54	7	<20	<65	ND
5R-1, 117–120	Troctolite	24	46.77	0.07	19.51	6.72	14.33	0.09	11.56	1.70	<0.02	<0.07	100.76	3.21	80.9	2.20	0.23	1163	14	<30	365	343	71	37	73	<1.5	<20	<65	ND
5R-2, 57–59	Ol-bearing gabbro	32	49.20	0.17	19.80	4.95	9.17	0.09	14.59	1.67	<0.04	<0.07	99.64	1.06	78.6	1.02	0.08	470	29	106	616	166	71	24	101	6	9	ND	<5
7G-1, 52–54	Cpx oikocryst-bearing ol gabbro	G23	47.60	0.13	20.08	5.98	12.20	0.09	13.05	1.58	0.01	<0.07	100.73	1.75	80.2	1.60	0.13	489	18	66	505	290	76	30	88	6	<5.5	ND	<5
8R-1, 79–85	Cpx oikocryst-bearing troctolite	38	47.76	0.14	19.16	4.89	11.96	0.08	14.52	1.28	<0.04	<0.07	99.80	2.02	82.9	1.76	0.22	392	25	90	784	254	81	14	88	2	18	<11.3	<21
8R-2, 110–112	Ol-bearing gabbro	42	47.28	0.11	19.78	4.45	13.05	0.08	14.18	1.33	0.04	<0.07	100.29	2.48	85.3	1.87	0.12	391	21	49	692	245	73	22	73	<1.5	<20	<65	ND
8R-3, 27–30	Cpx oikocryst-bearing troctolite	47	45.01	0.04	21.43	5.30	15.27	0.07	11.65	1.32	0.09	<0.07	100.18	3.46	85.1	2.94	0.30	312	3	<30	<19	330	79	32	86	<1.5	<20	<65	ND
8R-3, 33–35	Ol gabbro	48	49.77	0.18	16.30	4.02	12.51	0.09	16.60	1.60	<0.02	<0.07	101.07	2.28	86.0	1.41	0.40	186	43	124	525	182	69	21	68	3	<20	<65	ND
8R-3, 67–69	Ol-bearing gabbro	48	48.88	0.16	22.20	3.28	6.99	0.06	16.27	1.88	<0.04	<0.07	99.72	1.42	80.8	1.21	0.01	349	27	96	365	176	101	11	107	5	14	<11.3	<21
10R-1, 41–43	Troctolite	58	44.90	0.06	21.30	5.40	15.86	0.08	11.69	1.20	0.04	<0.07	100.53	2.67	85.3	2.34	0.12	389	4	<30	32	431	65	34	87	<1.5	<20	<65	ND
12R-1, 85–89	Gabbro	63	45.23	0.15	17.53	4.47	15.59	0.08	15.21	0.88	0.16	<0.07	99.31	5.26	87.4	4.37	0.06	163	30	72	2092	383	50	19	30	<1.5	<20	<65	ND
12R-1, 94–96	Ol gabbro	63	47.61	0.19	13.22	5.88	19.29	0.10	13.42	0.67	0.07	<0.07	100.45	4.38	86.7	3.84	0.15	1743	37	83	2481	489	66	25	16	4	<20	<65	ND
13R-1, 26–30	Ol-bearing anorthosite	66	44.79	0.02	26.77	2.32	6.70	0.06	15.61	1.29	0.26	<0.07	97.81	3.84	85.1	3.06	0.01	ND	<1	<30	392	260	17	35	168	<1.5	<20	<65	ND
13R-1, 38–44	Troctolite	66	42.52	0.03	11.68	8.75	29.86	0.12	7.18	0.15	0.05	<0.07	100.34	8.44	87.1	7.35	0.04	851	7	20	681	1488	120	42	34	<1.5	<5.5	<11.3	ND
18R-1, 67–72	Chromitite	70	31.01	0.02	13.13	30.53	22.78	0.04	3.96	0.34	<0.1	<0.07	101.82	6.72	59.6	6.51	0.08	ND	8	29	640	1180	11	18	1	<20	34	ND	<5
19R-1, 15–19	Troctolite	73	42.19	0.01	13.81	8.12	28.46	0.12	8.06	0.10	<0.1	<0.07	100.86	9.14	87.4	7.92	0.04	417	5	15	471	1207	28	42	40	<20	ND	<11.3	<5
21R-1, 56–60	Ol-bearing gabbro	78	45.04	0.13	24.09	5.94	12.66	0.08	11.49	1.87	0.15	<0.07	101.45	5.28	80.9	4.85	0.01	230	6	62	36	245	50	37	107	<20	39	ND	<5
21R-1, 116–124	Ol gabbro	78	46.72	0.16	23.77	4.79	10.79	0.07	13.06	2.06	0.09	<0.07	101.50	4.20	81.7	3.80	0.01	ND	12	70	111	231	37	29	121	<20	31	ND	8
23R-1, 50–53	Ol gabbro	85	47.18	0.12	25.26	4.30	9.36	0.06	13.07	2.20	<0.1	<0.07	101.61	3.72	81.2	3.50	0.03	ND	8	50	79	200	32	29	134	<20	26	ND	<5
25G-1, 35–37	Ol gabbro	G69	47.30	0.16	19.32	5.69	11.62	0.09	13.83	1.42	<0.1	<0.07	99.44	2.11	80.2	2.01	0.19	620	23	93	823	231	76	26	87	5	ND	<11.3	<5
345-U1415N-																													
2R-1, 3–5	Moderately ol phyric basalt	10	47.70	0.90	16.01	9.17	14.74	0.14	10.61	2.13	<0.04	<0.07	101.41	1.86	76.1	2.05	0.04	737	27	166	1138	534	62	52	55	21	39	<11.3	<21
4R-1, 12–15	Sparsely ol phyric basalt	13	49.32	1.19	17.86	9.19	8.19	0.14	11.81	2.91	<0.04	<0.07	100.61	2.63	63.8	2.66	0.05	381	43	252	449	164	71	52	95	27	55	<11.3	<21
345-U1415P-																													
3R-1, 31–34	Ol gabbro	2	46.26	0.14	22.85	5.13	10.92	0.07	13.52	1.30	<0.04	<0.07	100.20	3.11	80.8	2.90	0.20	287	10	55	586	277	53	19	102	4	8	<11.3	<21
3R-1, 120–124	Ol gabbro	3	50.05	0.25	17.92	5.77	10.52	0.10	14.77	1.70	<0.04	<0.07	101.08	1.66	78.3	1.62	0.05	800	36	130	814	206	76	19	82	11	7	<11.3	<21
4G-1, 41–44	Ol gabbro	G14	45.28	0.13	15.66	7.04	20.85	0.11	11.90	0.68	0.16	<0.07	101.81	4.30	85.4	4.17	0.11	424	18	63	1548	559	107	27	67	6	ND	ND	ND
5R-1, 37–41	Ol gabbro	3	46.21	0.19	23.71	4.72	9.84	0.07	14.05	1.24	0.15	<0.07	100.18	3.18	80.5	3.15	0.11	478	9	57	560	267	49	18	121	6	8	<11.3	<21
5R-2, 50–53	Ol gabbro	3	46.10	0.12	19.53	6.88	17.32	0.10	11.47	1.08	0.08	<0.07	102.69	4.10	83.3	3.97	0.13	388	10	37	452	442	78	34	91	4	8	ND	ND
6R-2, 90–93	Troctolitic ol gabbro	8	43.90	0.11	17.49	7.05	20.36	0.10	10.70	0.83	0.16	<0.07	100.70	4.77	85.1	4.54	0.14	549	10	46	1567	571	136	36	81	5	ND	ND	ND
7R-1, 112–115	Ol-bearing gabbro	13	47.94	0.23	16.37	4.78	13.57	0.10	16.06	1.40	0.19	<0.07	100.65	2.88	84.9	2.82	0.03	243	35	122	2558	277	53	21	99	5	<2	ND	ND
8R-1, 3–6	Ol gabbro	16	45.74	0.11	22.01	5.22	13.01	0.08	12.78	1.36	0.09	<0.07	100.38	3.20	83.2	3.09	0.19	ND	11	41	251	319	87	28	106	4	<2	ND	ND
9R-1, 4–7	Opx-bearing ol gabbro	18	45.02	0.18	21.25	5.54	13.23	0.07	11.33	1.52	0.08	<0.07	98.22	3.87	82.5	3.77	0.16	320	11	45	222	339	86	37	92	3	<2	ND	ND
9R-2, 19–23	Opx-bearing ol gabbro	21	45.47	0.11	18.66	6.79	18.47	0.10	11.57	0.97	0.14	<0.07	102.30	3.88	84.3	3.85	0.20	191	13	38	303	459	82	56	89	4	<2	ND	ND
11R-1, 42–46	Ol gabbro	25	45.90	0.13	18.90	6.96	17.99	0.11	11.18	1.09	0.15	<0.07	102.40	3.30	83.7	3.32	0.14	317	12	42	150	437	83	43	89	<1.8	<2	ND	ND
12R-1, 5–8	Opx-bearing ol gabbro	25	46.69	0.16	18.40	6.80	16.92	0.11	11.89	1.19	0.12	<0.07	102.28	2.59	83.1	2.68	0.16	464	18	63	438	361	96	44	85	5	<2	ND	ND
14R-1, 36–38	Ol gabbro	27	46.01	0.17	19.50	6.24	15.58	0.10	12.58	1.23	0.10	<0.07	101.50	2.68	83.2	2.78	0.19	225	16	63	670	370	91	37	84	4	<2	ND	ND
16R-1, 45–47	Troctolite	29	43.46	0.01	18.61	6.56	22.12	0.09	10.48	0.60	0.23	<0.07	102.15	5.13	87.0	5.20	0.05	231	3	ND	120	758	68	38	90	<1.8	<2	ND	ND
18R-1, 31–34	Troctolite	29	42.82	0.04	11.77	8.58	30.76	0.12	8.25	0.17	0.09	<0.07	102.60	7.67	87.7	7.60	0.09	266	9	21	931	1069	88	41	39	<1.8	<2	ND	ND
18R-1, 38–41	Troctolite	29	44.16	0.04	21.09	4.80	18.03	0.07	12.35	0.62	0.27	<0.07	101.42	6.58	88.2	6.41	0.03	312	5	14	409	708	71	27	100	2	<2	ND	ND
20R-1, 66–69	Troctolite	29	42.55	0.03	13.34	7.53	29.54	0.12	8.06	0.21	0.09	<0.07	101.46	9.69	88.6	9.57	0.03	352	8	23	1065	1168	83	46	46	2	<2	ND	ND
20R-2, 48–52	Troctolite	29	43.20	0.04	17.64	5.73	22.19	0.09	12.39	0.30	0.11	<0.07	101.67	8.69	88.5	8.24	0.04	161	7	18	681	856	53	40	50	3	<2	ND	ND

Inductively coupled plasma–atomic emission spectroscopy was used for determining major and trace element concentrations. Gas chromatography was used for determining H_2O and CO_2 content. Geochemical data are reported on a volatile-free basis for major and trace elements. LOI = loss on ignition. Mg# = 100 × cationic Mg/(Mg + Fe) with Fe = all Fe as Fe^{2+}. Ol = olivine, Opx = orthopyroxene, Cpx = clinopyroxene. ND = not determined.